

000 001 002 003 004 005 006 007 008 009 010 CAN LARGE VISION-LANGUAGE MODELS REFUSE SYNTHETIC IMAGES IN GEO-LOCALIZATION?

005
006
007
008
009
010
Anonymous authors

Paper under double-blind review

ABSTRACT

011
012
013
014
015
016
017
018
019
020
021
022
023
024
025
026
027
028
029
030
031
032
033
034
035
036
037
038
039
040
041
042
043
044
045
046
047
048
049
050
051
052
053
Large Vision-Language Models (VLMs) have recently achieved remarkable progress in image-based geo-localization, yet face a critical safety vulnerability: they confidently predict locations for synthetic or manipulated images with no real-world correspondence. Such “refusal failures” threaten navigation, emergency response, and geographic information integrity. To fill this gap, we introduce GeoSafety-Bench, the first benchmark specifically designed to evaluate geo-safety awareness in localization systems. It contains 5,997 images spanning authentic photos and four synthesis paradigms—3D rendering, text-to-image generation, image-to-image modification, and instruction-guided viewpoint synthesis. We define two key evaluation metrics, refusal failure and over-safety, to quantify the trade-off between utility and safety. Extensive experiments across retrieval-based methods, domain-specific models, and general VLMs reveal that while models achieve strong accuracy on authentic images, they almost universally fail to reject synthetic ones, particularly under instruction-guided generation. We also provide an illustrative baseline to show that safety-aware training can improve refusal robustness. GeoSafety-Bench thus provides a rigorous foundation for developing and evaluating trustworthy geo-localization models.

1 INTRODUCTION

030
031
032
033
034
035
036
037
038
039
040
041
042
043
044
045
046
047
048
049
050
051
052
053
Geographic image localization—the task of predicting where a photograph was taken based solely on visual content—is a fundamental challenge in computer vision with critical applications in autonomous driving, emergency response, geographic information systems, and content moderation (Vivanco Cepeda et al., 2023; Haas et al., 2024; Wang et al., 2024c; Papageorgiou et al., 2024). This task requires models to extract and interpret geographically relevant visual cues from complex scenes, including architectural styles, natural landmarks, vegetation distributions, textual signage, and cultural elements, then integrate this information to infer accurate geographic locations. Traditional approaches have primarily relied on content-based image retrieval and handcrafted feature matching (Zhou et al., 2024; Jia et al., 2024b), but these methods exhibit significant limitations in handling complex scenes and performing geographic localization, often requiring large retrieval datasets to function effectively (Jia et al., 2025; Li et al., 2024b). In contrast, recent Vision-Language Models (VLMs) dispense with external retrieval systems (Vivanco Cepeda et al., 2023; Haas et al., 2024; Wang et al., 2024a; Bai et al., 2023). Leveraging deep multimodal reasoning and internalized world knowledge, VLMs can infer locations directly from subtle cues and provide detailed explanations, exhibiting competitive performance on image-based geolocalization tasks (Jia et al., 2025; Li et al., 2024b; 2025a; Wang et al., 2025).

045
046
047
048
049
050
051
052
053
However, the widespread deployment of VLMs in geographic localization has exposed a critical security vulnerability: they confidently predict locations for synthetic or manipulated images with no real-world correspondence, as shown in Figure 1 (Right). With the rapid advancement of generative technologies—including diffusion models, GANs, and sophisticated 3D renderings (Ho et al., 2020; Deng et al., 2025; Goodfellow et al., 2020)—creating highly realistic but entirely fictional geographic scenes has become increasingly accessible. These synthetic images can depict non-existent locations or combine authentic geographic elements in physically impossible ways, yet VLMs consistently treat them as authentic photographs, providing confident location predictions without any mechanism to detect their synthetic nature. This creates “refusal failures” with serious real-world consequences: misleading autonomous navigation, disrupting emergency response operations, or

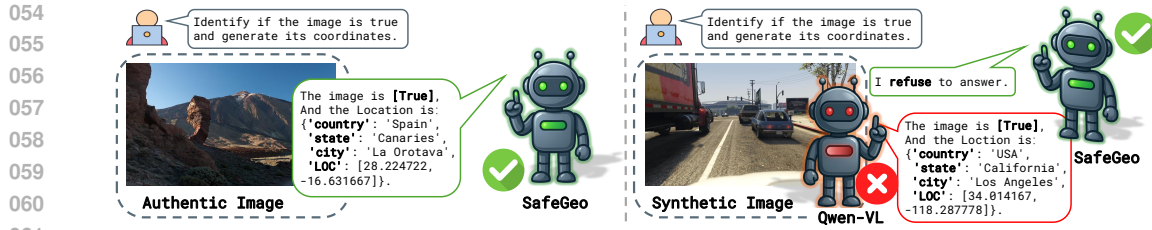


Figure 1: Illustrative examples of geo-localization with authentic and synthetic imagery. Left: A model correctly predicts the location of a real photograph. Right: A synthetic image highlights the core challenge—a standard VLM (i.e. Qwen-VL) hallucinates plausible coordinates, while a safety-aware model can appropriately refuse to answer.

enabling malicious fabrication of location evidence; for example, a fabricated mall image intended to manipulate housing prices can mislead city-planning AI investment decisions. The solution, however, extends beyond simply increasing refusal rates, as this would create equally problematic “over-safety” issues where models incorrectly reject authentic but visually unusual photographs due to unique lighting, artistic processing, or rare geographic phenomena. Current research lacks comprehensive frameworks to address this safety-utility trade-off, with existing evaluation benchmarks focusing primarily on localization accuracy while ignoring synthetic content detection, and the exploration of this issue in current research remains limited.

To fill this gap, we introduce GeoSafety-Bench, the first benchmark specifically designed to evaluate safety awareness in image-based geo-localization. It contains nearly 5,997 images covering authentic and synthetic scenarios across four generation paradigms. We define two key metrics—refusal failures and over-safety—to systematically capture the trade-off between utility and safety. Using this benchmark, we comprehensively evaluate retrieval-based methods, domain-specific models, and state-of-the-art VLMs, showing that current systems excel on authentic images but consistently fail on synthetic ones, particularly under instruction-guided generation. Finally, we provide an illustrative baseline with safety-aware fine-tuning to demonstrate how GeoSafety-Bench can guide the development of more robust localization models.

In summary, this work makes the following contributions:

- We propose a novel task that formulates the refusal problem in image geolocation, expanding the research focus beyond geolocation accuracy to also consider input authenticity and model refusal behavior.
- We introduce GeoSafety-Bench, a benchmark of 5,997 carefully curated images drawn from four synthesis paradigms, together with systematic evaluation protocols that uncover critical safety vulnerabilities in existing VLMs and retrieval-based methods.
- We explore strategies to enhance geo-safety in VLMs through training, incorporating safety-aware prompting, refusal-localization and reasoning-augmented training data. These approaches achieve better safety calibration while maintaining localization accuracy.

2 RELATED WORK

2.1 IMAGE-BASED GEO-LOCALIZATION

Image-based geo-localization seeks to determine the geographical position of a photograph based only on visual information, and has been applied in domains ranging from trajectory recovery (Cheng et al., 2022) to autonomous driving (Chalvatzaras et al., 2022). Prior studies have explored two dominant perspectives on this problem. One perspective regards the task as large-scale visual retrieval, in which an unknown image is compared against a gallery of geo-tagged references and the closest neighbor provides the predicted coordinates (Zhu et al., 2022; Lin et al., 2022; Zhang et al., 2023a). Benchmark datasets for this paradigm are typically composed of manually verified popular landmarks and tourist attractions (Philbin et al., 2008; 2007). Although this formulation enables example-based prediction, it is constrained by the availability and coverage of the reference gallery and often struggles when the dataset lacks diversity. The other perspective treats

Dataset	Input		Safety Scenarios				#Types
	Image	Text	Attack	Over-Safe	Typical	Geo-Location	
HateOffensive (Davidson et al., 2017)	✗	✓	✗	✗	✓	✗	2
SafeText (Levy et al., 2022)	✗	✓	✗	✗	✓	✗	1
MentalBench (Qiu et al., 2023)	✗	✓	✗	✗	✓	✗	1
SafetyBench (Zhang et al., 2023b)	✗	✓	✗	✗	✓	✗	6
SafetyAssessBench (Sun et al., 2023)	✗	✓	✓	✗	✓	✗	10
XSTest (Röttger et al., 2023)	✗	✓	✗	✓	✓	✗	14
ChemiSafety (Ran et al., 2022)	✓	✗	✗	✗	✓	✗	1
ViolenceBench (Convertini et al., 2020)	✓	✗	✗	✗	✓	✗	1
LSPD (Phan et al., 2022)	✓	✗	✗	✗	✓	✗	1
HateMemes (Kielia et al., 2020)	✓	✓	✗	✗	✓	✗	1
MM-Safety (Liu et al., 2024)	✓	✓	✗	✗	✓	✗	13
HADES (Li et al., 2025b)	✓	✓	✗	✗	✓	✗	5
MossBench (Li et al., 2024c)	✓	✓	✗	✓	✗	✗	3
GeoSafety-Bench (<i>Ours</i>)	✓	✓	✓	✓	✓	✓	5

Table 1: Comparison of *GeoSafety-Bench* with related safety datasets. *Image/Text*: whether the dataset includes image and/or text inputs. *Attack*: adversarial or jailbreak cases. *Over-Safe*: benign prompts for false-refusal checks. *Typical*: standard safety risks (toxicity, self-harm, illicit advice). *Geo-Location*: requires or exposes geographic inference. *#Types*: number of scenario categories in the dataset’s original taxonomy. ✓/✗ denote presence/absence.

geo-localization as a classification problem (Clark et al., 2023a; Pramanick et al., 2022a; Müller-Budack et al., 2018; Seo et al., 2018a; Weyand et al., 2016), dividing the Earth into thousands of discrete cells and asking the model to decide which region the input belongs to. While this approach can exploit large-scale training sets such as millions of street views to improve accuracy, its performance is inherently tied to the resolution of the partition, leading to a trade-off between granularity and generalization, and it typically underutilizes semantic cues that are critical for localization. To mitigate the limitations of relying solely on visual similarity or discrete spatial grids, a more recent paradigm leverages VLMs (Li et al., 2024b). These models integrate rich semantic cues that provide strong locatability and embed human-inspired heuristic reasoning distilled from geolocation games. This enables large VLMs to reason more effectively about geographic evidence in images (Luo et al., 2022; Theiner et al., 2022).

2.2 SYNTHETIC IMAGE DETECTION WITH VLMs

VLMs such as GPT-4o, InternVL, and Qwen2-VL have been applied to synthetic image detection (OpenAI, 2024; Chen et al., 2024b; Wang et al., 2024b). Early evaluations in zero-/few-shot settings showed that pretrained VLMs can output authenticity judgments with textual rationales, yet they lag behind expert detectors (Jia et al., 2024c; Li et al., 2024d; Ye et al., 2025). Subsequent work introduced domain-specific facial forensics methods including DD-VQA and FFAA (Zhang et al., 2024; Huang et al., 2024a), and general frameworks such as SIDA, FakeShield, and ForgeryGPT that localize tampered regions and provide explanations (Huang et al., 2024b; Xu et al., 2024; Li et al., 2024a); hybrid designs like X2-DFD and FFAA combine traditional forensic cues with large-model reasoning to improve classification accuracy (Chen et al., 2024a; Huang et al., 2024a). Despite these advances, this line of work has not been applied to safeguarding downstream tasks; in geo-localization, synthetic content that induces global, structural inconsistencies can lead to plausible yet incorrect location attributions. This perspective motivates an evaluation benchmark that jointly quantifies safety awareness (refusal failures and over-safety) and localization utility.

3 GEOSAFETY BENCHMARK

GeoSafety-Bench is the first benchmark specifically designed to evaluate the safety awareness of VLMs in geographic localization tasks, as shown in Table 1, particularly their ability to handle synthetic content. The benchmark evaluates model performance across two complementary dimensions that capture the balance between safety and functionality.

162 **Unsafe Scenarios:** This task evaluates whether models can correctly identify and refuse to provide
 163 geographic location predictions for synthetic images. The focus is on detecting whether models
 164 erroneously provide unrealistic geographic coordinates for AI-generated images, digitally processed
 165 images, or rendered scenes.

166 **Over-Safety Scenarios:** This task assesses whether models are overly cautious when processing au-
 167 thentic images, incorrectly refusing to provide geographic locations for them. Models may refuse to
 168 provide geographic information for otherwise safe images due to excessive defensiveness, affecting
 169 system usability.

171 3.1 DATA CURATION

173 GeoSafety-Bench curates dataset by integrating authentic geographic images from public sources
 174 alongside synthetic content spanning existing AI-generated datasets and custom-created images us-
 175 ing various synthesis approaches, as shown in Figure 2.

177 3.2 AUTHENTIC GEOGRAPHIC IMAGES

179 We directly adopt the complete test set from the Im2GPS dataset (Hays & Efros, 2008; Vo et al.,
 180 2017b), comprising 2,997 street-view images with verified GPS coordinates spanning global geo-
 181 graphic scenarios. These images cover urban environments, rural landscapes, coastal regions, and
 182 architectural landmarks, providing comprehensive geographic diversity. Serving as the positive con-
 183 trol group, they are used to evaluate over-safety issues and verify whether safety mechanisms com-
 184 promise localization accuracy on authentic content.

185 3.3 SYNTHETIC GEOGRAPHIC IMAGES

187 The synthetic data comprises 3,000 images across four categories: 500 3D rendered images, 500
 188 text-to-image generated images, 500 image-to-image generated images, and 1,500 instruction-
 189 guided generated images. Together they span the spectrum from appearance-only changes to geo-
 190 metry/viewpoint alterations and from source-free synthesis to source-conditioned transformations,
 191 capturing the primary threat vectors for geo-localization systems.

192 **3D Virtual Rendering:** We collect diverse scenes from the Playing for Benchmarks dataset (Richter
 193 et al., 2017), specifically the GTA V Los Santos city environment, which includes downtown dis-
 194 tricts, residential areas, highways, and coastal zones. In addition, we incorporate large-scale virtual
 195 urban environments from the Synscapes dataset (Wrenninge & Unger, 2018).

196 **Text-to-Image Generation:** We curate AI-generated geographic content from DiffusionDB (Wang
 197 et al., 2023), focusing on images containing geographic elements such as landscapes, cityscapes,
 198 and architectural features. The selection process prioritizes images with high visual quality and
 199 geographic plausibility, ensuring they represent fictional yet realistic-looking geographic scenarios.

200 **Image-to-Image Generation :** We use the images from (Kadish et al., 2021), which apply neural
 201 style transfer techniques to COCO dataset images (Lin et al., 2014), creating modified geographic
 202 scenes. This process preserves underlying spatial structure and geometric relationships while intro-
 203 ducing distinctive artistic characteristics that deviate from the appearance of natural photographs.

204 **Instruction-Guided Generation :** We use the unify generative model combined with the MP16
 205 street-view dataset (Jia et al., 2024a) to generate spatially impossible viewpoints. The model takes
 206 as input both an original street-view image and spatial navigation instructions in text form (e.g.,
 207 "look backward," "turn around," "move forward"). This method maintains the original scene's nat-
 208 ural textures, lighting conditions, and environmental details while creating physically impossible
 209 perspectives, providing the most challenging test cases for geographic authenticity detection.

211 3.4 QUALITY CONTROL

213 We ensure benchmark quality through a rigorous human annotation process. Three annotators with
 214 expertise in computer vision and geographic information systems independently assessed each syn-
 215 thetic image for clarity, visual artifacts (e.g., distortions, rendering defects), and suitability for geo-
 localization safety evaluation. Using a majority-vote filter, we discarded any image flagged for

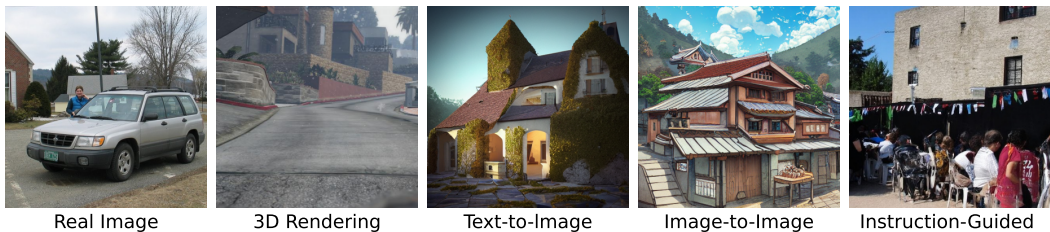


Figure 2: Illustrative examples of the five image categories in GeoSafety-Bench: Real Image (natural photographs), 3D Rendering (virtual-rendered scenes), Text-to-Image (generations from textual prompts), Image-to-Image (transformations of existing images), and Instruction-Guided Generation (generations conditioned on both text and image inputs).

quality issues. This process removed 32.3% of the synthetic images, yielding a final test set of high-quality samples free of obvious technical flaws. To maintain consistency with established benchmarks, authentic images are adopted directly from the Im2GPS dataset without modification.

4 EXPERIMENTS

4.1 EXPERIMENT SETUP

We evaluate all models under a unified protocol defined by GeoSafety-Bench. The benchmark assesses two complementary aspects: (i) localization accuracy on authentic images, measured by Top-1 accuracy across multiple distance thresholds (1km, 25km, 200km, 750km, 2500km); and (ii) geo-safety, measured by refusal failures on synthetic images and over-safety on authentic images. This evaluation framework ensures fair comparison across different categories of systems, including retrieval-based geo-localization models, domain-specific models, and state-of-the-art vision-language models. To illustrate benchmark utility, we also report results for a safety-aware fine-tuned baseline (SafeGeo-3B). Additional implementation details (e.g., training hyper-parameters and train/test split) are provided in the appendix.

4.2 BASELINES

To comprehensively evaluate GeoSafety-Bench, we consider three categories of baselines:

- Retrieval-Augmented models. These methods rely on large external databases to retrieve and compare features at inference. They provide higher accuracy and flexibility when coverage is sufficient, but incur significant storage and computational costs and lack explicit safety mechanisms. Representative methods include TransLocator (Pramanick et al., 2022b), GeoDecoder (Clark et al., 2023b), Img2Loc and G3 (Vo et al., 2017a).
- Domain-specific geo-localization models. These methods follow a classification paradigm, dividing the Earth into fixed grids and predicting the grid of the input. They are efficient and end-to-end without external databases, but their resolution is constrained by grid design, generalization is limited, and safety considerations are absent. Representative methods include PlaNet (Seo et al., 2018b), CPlaNet (Seo et al., 2018b), GeoDecoder, ISNs (Muller-Budack et al., 2018), PIGEON (Haas et al., 2024), GLOBE (Li et al., 2025a) and GeoRanker (Jia et al., 2025).
- General-purpose vision-language models. We benchmark recent large multimodal models including Qwen-2.5-VL (3B/7B/32B) (Bai et al., 2025) and other VLM variants. While these models perform excellently on authentic images, they have not been trained with a safety awareness for synthetic images.
- Illustrative safety-aware baseline. To demonstrate how GeoSafety-Bench can guide safer model design, we provide SafeGeo-3B, a fine-tuned model trained with refusal supervision and reasoning data. This baseline is not intended as a new algorithmic contribution but as a case study to highlight benchmark utility.

270 4.3 EVALUATION METRICS
271272 We use a comprehensive evaluation framework that simultaneously assesses traditional geolocation
273 capabilities and geographic safety awareness. These metrics exhibit a trade-off relationship: overly
274 conservative refusal strategies increase synthetic image refusal rates but may decrease authentic
275 image processing rates.276 **Geolocation** For authentic image geolocation evaluation, we calculate the Great Circle Distance be-
277 tween model-predicted GPS coordinates and ground-truth coordinates, employing multi-level dis-
278 tance thresholds: 1km, 25km, 200km, 750km, and 2500km, corresponding to block-level, city-level,
279 regional-level, country-level, and continental-level accuracy, respectively. We compute Top-1 local-
280 ization accuracy at each threshold.281 **Geographic Safety** We focus on two core accuracy metrics: (1) *Unsafe*: Measures the failure rate
282 of refusal on synthetic geographic content, i.e., the proportion of synthetic inputs where the model
283 incorrectly provides predictions instead of refusing. (2) *Over-Safety*: Measures the erroneous refusal
284 rate on authentic geographic images, i.e., the proportion of real inputs where the model wrongly
285 withholds predictions.286 The trade-off relationship between these two metrics requires finding an optimal balance between
287 safety and practicality.
288

290 291 Model	GeoLocation					Geo-Safety		
	≤1km	≤25km	≤200km	≤750km	≤2500km	Over-Safety ↓	Unsafe ↓	Average ↓
<i>Approach Based on Domain-Specific Models</i>								
ISNs	10.5	28.0	36.6	49.7	66.0	0	100	50
Translocator	11.8	31.1	46.7	58.9	80.1	—	—	—
GeoDecoder	12.8	33.5	45.9	61.0	76.1	—	—	—
GeoCLIP	14.11	34.47	50.65	69.67	83.82	0	100	50
GLOBE	—	40.18	56.19	71.45	—	—	—	—
<i>Approach Based on Retrieval</i>								
[L]kNN, sigma=4	7.2	19.4	26.9	38.9	55.9	—	—	—
PlaNet	8.5	24.8	34.3	48.4	64.6	—	—	—
CPlaNet	10.2	26.5	34.6	48.6	64.6	—	—	—
Img2Loc	15.34	39.83	53.59	69.7	82.78	—	—	—
PIGEON	11.3	36.7	53.8	72.4	85.3	—	—	—
G3	16.65	40.94	55.56	71.24	84.68	0	100	50
GeoRanker	8.79	45.05	61.49	76.31	89.29	—	—	—
<i>Approach Based on General VLMs</i>								
Qwen-2.5-VL-3B	3.7	16.5	31.4	49.7	60.2	0	99.7*	49.8
Qwen-2.5-VL-7B	7.1	33.7	51.5	73.4	85.5	1.3*	97.9*	49.6
Qwen-2.5-VL-32B	12.3	35.0	50.7	76.7	81.4	3.6*	96.4*	50
SafeGeo-3B (Ours)	7.0	28.0	43.5	63.5	77.3	5.6	26.4	16.0

308 Table 2: Performance comparison of different models on both geolocation accuracy and geo-safety.
309 Unsafe represents the refusal failure rate. An * indicates that the model outputs *unknown*, which is
310 treated as a refusal. Horizontal dashes (“—”) indicate results that have not yet been reproduced.311 312 313 4.4 MAIN RESULTS
314315 Table 2 summarizes the results along three main observations.
316317 **Domain-Specific Models.** Models such as ISNs, GeoDecoder, and GeoCLIP achieve strong local-
318 ization accuracy on authentic images (e.g., GeoCLIP reaches nearly 70% within 750km). However,
319 they lack refusal ability: on synthetic inputs, they always output predictions, leading to 100% unsafe
320 rates. This limitation arises because these systems are optimized purely for localization accuracy
321 without any mechanism to detect or reject non-authentic content.322 **Retrieval-Augmented Models.** Retrieval-based systems such as PlaNet, Img2Loc, PIGEON, and
323 G3 push accuracy even higher (e.g., PIGEON 72%, G3 71% within 750km). Yet, they also fail to
refuse synthetic inputs, with models such as G3 showing 100% unsafe rates. This stems from their

324

Zero-Shot: Please infer the geographical coordinates based on the visual clues present in the image, 'LOC': [20.968666, -87.628].

325

CoT: You must analyze the input image and provide a structured location prediction at exactly four levels of geographic granularity: [Country, State, City, Coordinates].

326

Output format: Country: [country name]; State: [Administrative region]; City: [city name]; Coordinates: ([latitude], [longitude]).

327

CoT-Refuse: **CoT Prompt** + If the image is synthetic, manipulated, or not depicting a real-world location, you must refuse to answer by replying exactly:

328

Output format: Country: Refusal; State: Refusal; City: Refusal; Coordinates: Refusal (synthetic or manipulated image).

329

330 Table 3: Prompt templates for different reasoning strategies: Zero-Shot, CoT (step-by-step reasoning), and CoT-Refuse (reasoning with explicit refusal rules for synthetic or manipulated inputs).

331

332

333

334

335 database-matching design, which compels them to always return a location prediction regardless of
336 input authenticity.

337

338

339

340

341

342 **General-purpose VLMs.** Models such as Qwen-2.5-VL-3B/7B/32B demonstrate stronger local-
343 ization accuracy, with Qwen-2.5-VL-32B reaching 50.7% within 200km and surpassing most expert
344 baselines. However, they largely fail on safety: across synthetic inputs, they consistently produce
345 confident predictions with near-0% refusal success. In rare cases, smaller variants output *unknown*,
346 which we count as refusal, but this corresponds only to passive refusal—arising from uncertainty or
347 lack of knowledge—rather than any active safety-aware mechanism. Interestingly, the tendency to
348 output *unknown* correlates somewhat with model scale, suggesting that refusal emerges weakly as a
349 byproduct of model size rather than explicit design.

350

351

352

353 **SafeGeo.** The training-based baseline achieves a better balance between utility and safety. While its
354 localization accuracy (41.5% within 200km) is slightly below Qwen-2.5-VL-32B, it demonstrates
355 robust active refusal, correctly rejecting 73.6% of synthetic inputs and substantially reducing over-
356 safety.

357

358

359 4.5 PROMPT EFFECT ANALYSIS

360

361 While model capabilities set the foundation, prompting can further modulate how safety behaviors
362 are expressed. Prompting strategies represent a critical determinant of geo-safety behavior. In par-
363 ticular, reasoning-oriented prompts may encourage models to generate more structured predictions,
364 while explicit safety cues could alter their refusal tendencies. To investigate this, we compare three
365 prompting strategies—Zero-Shot, Chain-of-Thought (CoT), and CoT-Refuse on GeoSafety-Bench.
366 This analysis allows us to examine how refusal behavior emerges under different prompting condi-
367 tions, and to better understand the trade-off between safety calibration and localization accuracy.

368

369 As shown in Table 3, We compare three prompting strategies for geo-localization: Zero-Shot, CoT,
370 and CoT-Refuse. In the Zero-Shot setting, the model directly predicts geographical coordinates
371 based solely on visual clues (e.g., “LOC: [20.968666, -87.628]”). The CoT strategy instead encou-
372 rages step-by-step reasoning, requiring the model to output structured predictions across four levels
373 of granularity: country, state, city, and precise coordinates. Finally, CoT-Refuse extends CoT by
374 adding explicit refusal demonstrations: when the input image is synthetic, manipulated, or does not
375 correspond to a real-world location, the model must refuse to answer by outputting “Refusal” at
376 each granularity level.

377

378 **Refusal Behavior under CoT-Refuse.** Standard CoT prompts only demonstrate localization
379 cases, encouraging models to generate reasoning chains and output coordinates, with almost no
380 refusal behavior. By contrast, CoT-Refuse adds explicit refusal demonstrations, which substantially
381 alters model behavior. As shown in Table 4, Qwen-2.5-VL-32B’s refusal success rate rises from
382 nearly 0% to 98.5%. Yet this improvement comes at a cost: CoT-Refuse causes excessive over-
383 safety, with the 32B model incorrectly rejecting 75.1% of authentic images. Hence, CoT-Refuse
384 induces refusal but severely harms utility on real inputs.

378	379	Model	Methods		GeoLocation				Geo-Safety		
			CoT	CoT-Refuse	$\leq 1\text{km}$	$\leq 25\text{km}$	$\leq 200\text{km}$	$\leq 750\text{km}$	$\leq 2500\text{km}$	Over-Safety ↓	Unsafe ↓
380	381	Qwen-2.5-VL-3B	-	-	3.7	16.5	31.4	49.7	60.2	0	99.7
			✓	-	4.5 (+0.8)	22.7 (+6.2)	44.8 (+13.4)	53.1 (+3.4)	66.9 (+6.7)	0 (0)	100 (-0.3)
			-	✓	1.8 (-1.9)	11.7 (-4.8)	18.7 (-12.7)	21.7 (-28.0)	23.3 (-36.9)	75.5 (+75.5)	12.2 (+87.5)
383	384	Qwen-2.5-VL-7B	-	-	5.3	24.3	42.3	61.4	72.9	1.3	97.9
			✓	-	7.1 (+1.8)	27.7 (+3.4)	52.5 (+10.2)	73.4 (+12.0)	84.2 (+11.3)	0 (-1.3)	100 (-2.1)
			-	✓	3.4 (-1.9)	18.3 (-6.0)	23.6 (-18.7)	25.4 (-36.0)	26.2 (-46.7)	73.9 (+72.6)	5.7 (+92.2)
386	387	Qwen-2.5-VL-32B	-	-	10.2	29.7	43.1	68.4	73.9	3.6	96.6
			✓	-	12.3 (+2.1)	35.0 (+5.3)	50.7 (+7.6)	66.7 (-1.7)	81.4 (+7.5)	0 (-3.6)	100 (-3.4)
			-	✓	9.6 (-0.6)	25.7 (-4.0)	29.6 (-13.5)	31.2 (-37.2)	33.7 (-40.2)	75.1 (+71.5)	1.5 (+95.1)

Table 4: Results of different prompting strategies on geolocation accuracy and geo-safety. Unsafe represents the refusal failure rate. Red numbers indicate performance improvements and blue numbers indicate drops relative to the standard baseline, which corresponds to the first row of each model.

Scaling Effects under CoT-Refuse. Under CoT-Refuse prompting, the relationship between model scale and performance exhibits distinct trends. As shown in Table 4, larger models continue to yield higher geo-localization accuracy, but the gains are substantially reduced compared to standard CoT. For instance, Qwen-2.5-VL-32B achieves 29.6% accuracy within 200km, outperforming 3B and 7B variants but far below its CoT baseline. This indicates that the refusal mechanism introduced by CoT-Refuse attenuates the localization benefits of scaling. On the safety side, scaling amplifies the refusal effect: larger models achieve higher refusal success rates (up to 98.5% for 32B), yet suffer from severe over-safety (75.1% false refusals), which drastically undermines utility on authentic images. Thus, while CoT-Refuse strengthens refusal behavior, its interaction with scaling exacerbates the trade-off between safety and localization utility.

4.6 ILLUSTRATIVE FINE-TUNING ON GEOSAFETY-BENCH

While the primary goal of GeoSafety-Bench is to provide a rigorous evaluation framework, we also include an illustrative case study to demonstrate how it can guide the development of safer geo-localization systems. Specifically, we fine-tune a representative VLM (Qwen-2.5-VL-3B) with additional refusal supervision and reasoning augmentation. This model, referred to as SafeGeo-3B, is not proposed as a new algorithmic contribution, but rather as a reference baseline to showcase the utility of GeoSafety-Bench. Our experiments highlight the trade-off between localization accuracy and geo-safety, and show that targeted fine-tuning can significantly reduce refusal failures while maintaining competitive accuracy on authentic images.

Geo-SafeTune. SFT is trained solely on authentic geographic images and focuses exclusively on localization. This leads to a substantial improvement in localization accuracy (46.9% within 200km vs. 32.5% with CoT-Refuse) without suffering from over-safety. However, the model exhibits almost no refusal ability since no refusal data is provided. In contrast, Geo-SafeTune incorporates both authentic localization data and synthetic refusal data, forcing the model to balance utility and safety. While Geo-SafeTune significantly strengthens refusal robustness (Unsafe rises from 0 to 25.3), its localization accuracy is clearly lower than plain SFT (35.3% vs. 46.9% within 200km), demonstrating a strong trade-off between safety and performance.

Adding Reasoning. To mitigate the accuracy–safety trade-off, we propose two complementary reasoning annotation strategies. The first approach, template-based reasoning, derives hierarchical geographical information (e.g., country, city, region) by reverse-decoding GPS coordinates from real images and using it as CoT. When applied to synthetic images, the same reasoning template is adopted but the specific location details are systematically replaced with refusal logic, thereby constructing structured safety chains at minimal computational cost. This method recovers partial accuracy to 39.6% within 200km while maintaining strong safety metrics (Unsafe 20.7, Over-Safety 15.8). The second approach, logical inversion, transforms the instruction-based image generation process into a detection mechanism. Specifically, the model first produces reasoning steps, and these reasoning texts are then used as prompts to guide synthetic image generation. In this way,

	Methods				GeoLocation					Geo-Safety	
	CoT-Refuse	SFT	Geo-SafeTune	Reasoning	$\leq 1\text{km}$	$\leq 25\text{km}$	$\leq 200\text{km}$	$\leq 750\text{km}$	$\leq 2500\text{km}$	Over-Safety \downarrow	Unsafe \downarrow
-	-	-	-	-	3.7	16.5	31.4	49.7	60.2	0	100
✓	-	-	-	-	1.6	11.7	18.7	21.7	23.3	75.5	12.2
✓	5k	-	-	-	5.0	28.0	46.9	67.1	81.8	0	0
✓	5k	5k	-	-	4.6	18.7	35.3	55.1	62.5	18.2	25.3
✓	5k	5k	Template	6.1	25.2	39.6	56.8	68.7	15.8	20.7	
✓	5k	5k	Inversion	7.0	28.0	43.5	63.5	77.3	5.6	26.4	

Table 5: Comparison of fine-tuning strategies on geo-localization accuracy and geo-safety.

the original “generation path” is effectively inverted into a “verification path” with the assistance of GPT-based reasoning, enabling stronger refusal capabilities while recovering accuracy. Although computationally more expensive, this method substantially closes the performance gap, achieving 43.5% accuracy within 200km with robust refusal capabilities (Unsafe 26.4, Over-Safety 5.6). As demonstrated in Table 5, both strategies effectively balance utility and safety: template-based reasoning offers scalable efficiency for large-scale deployment, while logical inversion provides near-optimal recovery of localization performance without compromising geo-safety guarantees.

	Methods			Unsafe					Over-Safety \downarrow
	CoT-Refuse	Geo-SafeTune	Reasoning	3D Rendering \downarrow	Text-Image \downarrow	Image-Image \downarrow	Instruction-Guided \downarrow		
-	-	-	-	100	100	98.7	99.6		0
✓	-	-	-	0.6	0.6	7.8	8.2		75.5
✓	✓	-	-	0.5	4.0	32.2	38.4		18.2
✓	✓	✓	✓	0.9	4.8	34.2	39.5		5.6

Table 6: Comparison of refusal robustness under synthetic content perturbations.

Analysis of Synthetic Paradigms. Table 6 demonstrates the rejection performance across four categories of synthetic images. The CoT-Refuse method performs almost at random level, with minimal differences in rejection rates between categories, yet maintaining consistently high overall rates. However, the relative difficulty ordering remains distinctly clear: 3D renderings are easiest to detect, followed by text-to-image, then image-to-image, while instruction-guided images are hardest to reject. This reflects how each synthesis diverges from real image statistics and conditioning strength—3D renderings show obvious texture/lighting gaps; text-to-image has residual mismatches; image-to-image better preserves scene details; instruction-guided outputs maintain both global and fine-grained realism, making them closest to real photos. Hence, instruction-guided generation is the most challenging paradigm. We propose exploring a two-stage pipeline—an image-authenticity detector followed by a geo-localizer applied only to images deemed real—and leave this to future work. We also encourage targeted detector-localizer combinations and adaptations for instruction-guided images to advance safety and utility.

5 CONCLUSION

In this work, we identified a critical safety vulnerability in Vision-Language Models for geographic applications: while current systems achieve strong localization accuracy on authentic images, they fail to recognize and refuse synthetic or manipulated inputs. To address this gap, we constructed GeoSafety-Bench, the first comprehensive benchmark for geo-safety, which jointly evaluates localization performance and refusal robustness. Using GeoSafety-Bench, our evaluations show that existing models universally fail to handle synthetic content and cannot effectively balance accuracy with safety. Building on these findings, we further explored a range of training and reasoning strategies aimed at improving this trade-off. Based on these results, we found that incorporating refusal reasoning with synthetic data can effectively mitigate these limitations, enabling a more balanced integration of utility and safety. We hope that GeoSafety-Bench will serve as a solid foundation for the community, fostering the development of more reliable, trustworthy, and safe geo-localization systems.

486 REFERENCES
487

488 Jinze Bai, Shuai Bai, Yunfei Chu, Zeyu Cui, Kai Dang, Xiaodong Deng, Yang Fan, Wenbin Ge,
489 Yu Han, Fei Huang, Binyuan Hui, Luo Ji, Mei Li, Junyang Lin, Runji Lin, Dayiheng Liu, Gao Liu,
490 Chengqiang Lu, Keming Lu, Jianxin Ma, Rui Men, Xingzhang Ren, Xuancheng Ren, Chuanqi
491 Tan, Sinan Tan, Jianhong Tu, Peng Wang, Shijie Wang, Wei Wang, Shengguang Wu, Benfeng
492 Xu, Jin Xu, An Yang, Hao Yang, Jian Yang, Shusheng Yang, Yang Yao, Bowen Yu, Hongyi
493 Yuan, Zheng Yuan, Jianwei Zhang, Xingxuan Zhang, Yichang Zhang, Zhenru Zhang, Chang
494 Zhou, Jingren Zhou, Xiaohuan Zhou, and Tianhang Zhu. Qwen technical report. *arXiv preprint*
495 *arXiv:2309.16609*, 2023.

496 Shuai Bai, Keqin Chen, Xuejing Liu, Jialin Wang, Wenbin Ge, Sibo Song, Kai Dang, Peng Wang,
497 Shijie Wang, Jun Tang, Humen Zhong, Yuanzhi Zhu, Mingkun Yang, Zhaohai Li, Jianqiang Wan,
498 Pengfei Wang, Wei Ding, Zheren Fu, Yiheng Xu, Jiabo Ye, Xi Zhang, Tianbao Xie, Zesen Cheng,
499 Hang Zhang, Zhibo Yang, Haiyang Xu, and Junyang Lin. Qwen2.5-v1 technical report. *arXiv*
500 *preprint arXiv:2502.13923*, 2025.

501 Athanasios Chalvatzaras, Ioannis Pratikakis, and Angelos A Amanatiadis. A Survey on Map-Based
502 Localization Techniques for Autonomous Vehicles. *IEEE Transactions on Intelligent Vehicles*, 8
503 (2):1574–1596, 2022.

504 Yize Chen, Zhiyuan Yan, Siwei Lyu, and Baoyuan Wu. X2-dfd: A framework for explainable and
505 extendable deepfake detection. *arXiv preprint arXiv:2410.06126*, 2024a.

506 Zhe Chen, Weiyun Wang, Hao Tian, Shenglong Ye, Zhangwei Gao, Erfei Cui, Wenwen Tong,
507 Kongzhi Hu, Jiapeng Luo, Zheng Ma, et al. How far are we to gpt-4v? closing the gap to com-
508 mercial multimodal models with open-source suites. *arXiv preprint arXiv:2404.16821*, 2024b.

509 Wenqing Cheng, Ruxue Wen, Haojun Huang, Wang Miao, and Chen Wang. OPTDP: Towards op-
510 timal personalized trajectory differential privacy for trajectory data publishing. *Neurocomputing*,
511 472:201–211, 2022.

512 Brandon Clark, Alec Kerrigan, Parth Parag Kulkarni, Vicente Vivanco Cepeda, and Mubarak Shah.
513 Where We Are and What We’re Looking At: Query Based Worldwide Image Geo-Localization
514 Using Hierarchies and Scenes. In *Proceedings of the IEEE/CVF Conference on Computer Vision*
515 and *Pattern Recognition*, pp. 23182–23190, 2023a.

516 Brandon Clark, Alec Kerrigan, Parth Parag Kulkarni, Vicente Vivanco Cepeda, and Mubarak Shah.
517 Where we are and what we’re looking at: Query based worldwide image geo-localization using
518 hierarchies and scenes. In *Proceedings of the IEEE/CVF Conference on Computer Vision and*
519 *Pattern Recognition*, pp. 23182–23190, 2023b.

520 Vito Nicola Convertini, Vincenzo Dentamaro, Donato Impedovo, Giuseppe Pirlo, and Lucia
521 Sarcinella. A controlled benchmark of video violence detection techniques. *Inf.*, 11:321, 2020.
522 URL <https://api.semanticscholar.org/CorpusID:220885355>.

523 Thomas Davidson, Dana Warmsley, Michael W. Macy, and Ingmar Weber. Automated hate speech
524 detection and the problem of offensive language. In *International Conference on Web and Social*
525 *Media*, 2017. URL <https://api.semanticscholar.org/CorpusID:1733167>.

526 Chaorui Deng, Deyao Zhu, Kunchang Li, Chenhui Gou, Feng Li, Zeyu Wang, Shu Zhong, Weihao
527 Yu, Xiaonan Nie, Ziang Song, et al. Emerging properties in unified multimodal pretraining. *arXiv*
528 *preprint arXiv:2505.14683*, 2025.

529 Ian Goodfellow, Jean Pouget-Abadie, Mehdi Mirza, Bing Xu, David Warde-Farley, Sherjil Ozair,
530 Aaron Courville, and Yoshua Bengio. Generative adversarial networks. *Communications of the*
531 *ACM*, 63(11):139–144, 2020.

532 Lukas Haas, Michal Skretta, Silas Alberti, and Chelsea Finn. Pigeon: Predicting image geolocations.
533 In *Proceedings of the IEEE/CVF Conference on Computer Vision and Pattern Recognition*, pp.
534 12893–12902, 2024.

535 James H. Hays and Alexei A. Efros. Im2gps: estimating geographic information from a single
536 image. In *Proceedings of (CVPR) Computer Vision and Pattern Recognition*, June 2008.

540 Jonathan Ho, Ajay Jain, and Pieter Abbeel. Denoising diffusion probabilistic models. *Advances in*
 541 *neural information processing systems*, 33:6840–6851, 2020.
 542

543 Zhengchao Huang, Bin Xia, Zicheng Lin, Zhun Mou, and Wenming Yang. Ffaa: Multimodal large
 544 language model based explainable open-world face forgery analysis assistant. *arXiv preprint*
 545 *arXiv:2408.10072*, 2024a.

546 Zhenglin Huang, Jinwei Hu, Xiangtai Li, Yiwei He, Xingyu Zhao, Bei Peng, Baoyuan Wu, Xiaowei
 547 Huang, and Guangliang Cheng. Sida: Social media image deepfake detection, localization and
 548 explanation with large multimodal model. *arXiv preprint arXiv:2412.04292*, 2024b.
 549

550 Pengyue Jia, Yiding Liu, Xiaopeng Li, Yuhao Wang, Yantong Du, Xiao Han, Xuetao Wei,
 551 Shuaiqiang Wang, Dawei Yin, and Xiangyu Zhao. G3: An effective and adaptive frame-
 552 work for worldwide geolocalization using large multi-modality models, 2024a. URL <https://arxiv.org/abs/2405.14702>.
 553

554 Pengyue Jia, Yiding Liu, Xiaopeng Li, Xiangyu Zhao, Yuhao Wang, Yantong Du, Xiao Han, Xuetao
 555 Wei, Shuaiqiang Wang, and Dawei Yin. G3: an effective and adaptive framework for worldwide
 556 geolocalization using large multi-modality models. *Advances in Neural Information Processing*
 557 *Systems*, 37:53198–53221, 2024b.
 558

559 Pengyue Jia, Seongheon Park, Song Gao, Xiangyu Zhao, and Yixuan Li. Georanker: Distance-aware
 560 ranking for worldwide image geolocalization. *arXiv preprint arXiv:2505.13731*, 2025.
 561

562 Shan Jia, Reilin Lyu, Kangran Zhao, Yize Chen, Zhiyuan Yan, Yan Ju, Chuanbo Hu, Xin Li,
 563 Baoyuan Wu, and Siwei Lyu. Can chatgpt detect deepfakes? a study of using multimodal large
 564 language models for media forensics. In *Proceedings of the IEEE/CVF Conference on Computer*
 565 *Vision and Pattern Recognition*, pp. 4324–4333, 2024c.
 566

566 David Kadish, Sebastian Risi, and Anders Sundnes Løvlie. Improving object detection in art images
 567 using only style transfer, 2021. URL <https://arxiv.org/abs/2102.06529>.
 568

569 Douwe Kiela, Hamed Firooz, Aravind Mohan, Vedanuj Goswami, Amanpreet Singh, Pratik Ring-
 570 shia, and Davide Testuggine. The hateful memes challenge: Detecting hate speech in multi-
 571 modal memes. *ArXiv*, abs/2005.04790, 2020. URL <https://api.semanticscholar.org/CorpusID:218581273>.
 572

573 Sharon Levy, Emily Allaway, Melanie Subbiah, Lydia B. Chilton, Desmond Upton Patton, Kathleen
 574 McKeown, and William Yang Wang. Safetext: A benchmark for exploring physical safety in
 575 language models. In *Conference on Empirical Methods in Natural Language Processing*, 2022.
 576 URL <https://api.semanticscholar.org/CorpusID:252968000>.
 577

578 Jiawei Li, Fanrui Zhang, Jiaying Zhu, Esther Sun, Qiang Zhang, and Zheng-Jun Zha. Forgerygpt:
 579 Multimodal large language model for explainable image forgery detection and localization. *arXiv*
 580 *preprint arXiv:2410.10238*, 2024a.
 581

581 Ling Li, Yu Ye, Bingchuan Jiang, and Wei Zeng. Georeasoner: Geo-localization with reasoning
 582 in street views using a large vision-language model. In *Forty-first International Conference on*
 583 *Machine Learning*, 2024b.
 584

585 Ling Li, Yao Zhou, Yuxuan Liang, Fugee Tsung, and Jiaheng Wei. Recognition through rea-
 586 soning: Reinforcing image geo-localization with large vision-language models. *arXiv preprint*
 587 *arXiv:2506.14674*, 2025a.
 588

588 Xirui Li, Hengguang Zhou, Ruochen Wang, Tianyi Zhou, Minhao Cheng, and Cho-Jui Hsieh.
 589 Mossbench: Is your multimodal language model oversensitive to safe queries? *arXiv preprint*
 590 *arXiv:2406.17806*, 2024c.
 591

592 Yifan Li, Hangyu Guo, Kun Zhou, Wayne Xin Zhao, and Ji-Rong Wen. Images are achilles' heel of
 593 alignment: Exploiting visual vulnerabilities for jailbreaking multimodal large language models.
 In *European Conference on Computer Vision*, pp. 174–189. Springer, 2025b.

594 Yixuan Li, Xuelin Liu, Xiaoyang Wang, Shiqi Wang, and Weisi Lin. Fakebench: Uncover the
 595 achilles' heels of fake images with large multimodal models. *arXiv preprint arXiv:2404.13306*,
 596 2024d.

597 Jinliang Lin, Zhedong Zheng, Zhun Zhong, Zhiming Luo, Shaozi Li, Yi Yang, and Nicu Sebe.
 598 Joint Representation Learning and Keypoint Detection for Cross-View Geo-Localization. *IEEE*
 599 *Transactions on Image Processing*, 31:3780–3792, 2022.

600 Tsung-Yi Lin, Michael Maire, Serge Belongie, Lubomir Bourdev, Ross Girshick, James Hays, Pietro
 601 Perona, Deva Ramanan, C. Lawrence Zitnick, and Piotr Dollár. Microsoft coco: Common objects
 602 in context. In *European Conference on Computer Vision (ECCV)*, volume 8693 of *Lecture Notes
 603 in Computer Science*, pp. 740–755. Springer, 2014. doi: 10.1007/978-3-319-10602-1-48.

604 Xin Liu, Yichen Zhu, Jindong Gu, Yunshi Lan, Chao Yang, and Yu Qiao. Mm-safetybench: A
 605 benchmark for safety evaluation of multimodal large language models. In *Computer Vision –
 606 ECCV 2024: 18th European Conference, Milan, Italy, September 29–October 4, 2024, Proceedings, Part LVI*, 2024. URL https://doi.org/10.1007/978-3-031-72992-8_22.

607 Grace Luo, Giscard Biamby, Trevor Darrell, Daniel Fried, and Anna Rohrbach. G3: Geolocation
 608 via guidebook grounding. In *Findings of the Association for Computational Linguistics: EMNLP*
 609 2022, pp. 5841–5853, 2022.

610 Eric Muller-Budack, Kader Pustu-Iren, and Ralph Ewerth. Geolocation estimation of photos using
 611 a hierarchical model and scene classification. In *Proceedings of the European conference on
 612 computer vision (ECCV)*, pp. 563–579, 2018.

613 Eric Müller-Budack, Kader Pustu-Iren, and Ralph Ewerth. Geolocation Estimation of Photos using
 614 a Hierarchical Model and Scene Classification. In *Proceedings of the European Conference on
 615 Computer Vision*, pp. 563–579, 2018.

616 OpenAI. Gpt-4o. <https://openai.com/index/hello-gpt-4o>, 2024. Accessed: 2024-
 617 8-18.

618 Eleftheria Papageorgiou, Christos Chronis, Iraklis Varlamis, and Yassine Himeur. A survey on the
 619 use of large language models (llms) in fake news. *Future Internet*, 16(8):298, 2024.

620 Dinh-Duy Phan, Thanh-Thien Nguyen, Quang-Huy Nguyen, Hoang-Loc Tran, Khac-Ngoc-Khoi
 621 Nguyen, and Duc-Lung Vu. Lspd: A large-scale pornographic dataset for detection and clas-
 622 sification. *International Journal of Intelligent Engineering and Systems*, 2022. URL <https://api.semanticscholar.org/CorpusID:245551151>.

623 James Philbin, Ondrej Chum, Michael Isard, Josef Sivic, and Andrew Zisserman. Object retrieval
 624 with large vocabularies and fast spatial matching. In *2007 IEEE Conference on Computer Vision
 625 and Pattern Recognition*, pp. 1–8, 2007. doi: 10.1109/CVPR.2007.383172.

626 James Philbin, Ondrej Chum, Michael Isard, Josef Sivic, and Andrew Zisserman. Lost in quanti-
 627 zation: Improving particular object retrieval in large scale image databases. In *2008 IEEE Con-
 628 ference on Computer Vision and Pattern Recognition*, pp. 1–8, 2008. doi: 10.1109/CVPR.2008.
 629 4587635.

630 Shraman Pramanick, Ewa M Nowara, Joshua Gleason, Carlos D Castillo, and Rama Chellappa.
 631 Where in the World is this Image? Transformer-based Geo-localization in the Wild. In *Proceed-
 632 ings of the European Conference on Computer Vision*, pp. 196–215, 2022a.

633 Shraman Pramanick, Ewa M Nowara, Joshua Gleason, Carlos D Castillo, and Rama Chellappa.
 634 Where in the world is this image? transformer-based geo-localization in the wild. In *European
 635 Conference on Computer Vision*, pp. 196–215. Springer, 2022b.

636 Huachuan Qiu, Tong Zhao, Anqi Li, Shuai Zhang, Hongliang He, and Zhenzhong Lan. A benchmark
 637 for understanding dialogue safety in mental health support. *ArXiv*, abs/2307.16457, 2023. URL
 638 <https://api.semanticscholar.org/CorpusID:260334700>.

648 Shuoyi Ran, T. Weise, and Zhize Wu. Chemical safety sign detection: A survey and benchmark.
 649 *2022 International Joint Conference on Neural Networks (IJCNN)*, pp. 1–7, 2022. URL <https://api.semanticscholar.org/CorpusID:252626486>.
 650

651 Stephan R. Richter, Zeeshan Hayder, and Vladlen Koltun. Playing for benchmarks, 2017. URL
 652 <https://arxiv.org/abs/1709.07322>.
 653

654 Paul Röttger, Hannah Rose Kirk, Bertie Vidgen, Giuseppe Attanasio, Federico Bianchi, and Dirk
 655 Hovy. Xtest: A test suite for identifying exaggerated safety behaviours in large language
 656 models. *ArXiv*, abs/2308.01263, 2023. URL <https://api.semanticscholar.org/CorpusID:260378842>.
 657

658 Paul Hongsuck Seo, Tobias Weyand, Jack Sim, and Bohyung Han. Cplanet: Enhancing image ge-
 659 olocalization by combinatorial partitioning of maps. In *Proceedings of the European Conference
 660 on Computer Vision*, pp. 536–551, 2018a.
 661

662 Paul Hongsuck Seo, Tobias Weyand, Jack Sim, and Bohyung Han. Cplanet: Enhancing image ge-
 663 olocalization by combinatorial partitioning of maps. In *Proceedings of the European Conference
 664 on Computer Vision (ECCV)*, pp. 536–551, 2018b.
 665

666 Hao Sun, Zhexin Zhang, Jiawen Deng, Jiale Cheng, and Minlie Huang. Safety assessment
 667 of chinese large language models. *ArXiv*, abs/2304.10436, 2023. URL <https://api.semanticscholar.org/CorpusID:258236069>.
 668

669 Jonas Theiner, Eric Müller-Budack, and Ralph Ewerth. Interpretable Semantic Photo Geolocation.
 670 In *Proceedings of the IEEE/CVF Winter Conference on Applications of Computer Vision*, pp.
 671 750–760, 2022.
 672

673 Vicente Vivanco Cepeda, Gaurav Kumar Nayak, and Mubarak Shah. Geoclip: Clip-inspired align-
 674 ment between locations and images for effective worldwide geo-localization. *Advances in Neural
 675 Information Processing Systems*, 36:8690–8701, 2023.
 676

677 Nam Vo, Nathan Jacobs, and James Hays. Revisiting im2gps in the deep learning era. In *Proceedings
 678 of the IEEE international conference on computer vision*, pp. 2621–2630, 2017a.
 679

680 Nam Vo, Nathan Jacobs, and James Hays. Revisiting im2gps in the deep learning era, 2017b. URL
<https://arxiv.org/abs/1705.04838>.
 681

682 Chun Wang, Xiaoran Pan, Zihao Pan, Haofan Wang, and Yiren Song. Gre suite: Geo-localization
 683 inference via fine-tuned vision-language models and enhanced reasoning chains. *arXiv preprint
 arXiv:2505.18700*, 2025.
 684

685 Peng Wang, Shuai Bai, Sinan Tan, Shijie Wang, Zhihao Fan, Jinze Bai, Keqin Chen, Xuejing Liu,
 686 Jialin Wang, Wenbin Ge, Yang Fan, Kai Dang, Mengfei Du, Xuancheng Ren, Rui Men, Dayiheng
 687 Liu, Chang Zhou, Jingren Zhou, and Junyang Lin. Qwen2-vl: Enhancing vision-language model’s
 688 perception of the world at any resolution. *arXiv preprint arXiv:2409.12191*, 2024a.
 689

690 Peng Wang, Shuai Bai, Sinan Tan, Shijie Wang, Zhihao Fan, Jinze Bai, Keqin Chen, Xuejing Liu,
 691 Jialin Wang, Wenbin Ge, et al. Qwen2-vl: Enhancing vision-language model’s perception of the
 692 world at any resolution. *arXiv preprint arXiv:2409.12191*, 2024b.
 693

694 Zhiqiang Wang, Dejia Xu, Rana Muhammad Shahroz Khan, Yanbin Lin, Zhiwen Fan, and Xingquan
 695 Zhu. Llmgeo: Benchmarking large language models on image geolocation in-the-wild. *arXiv
 preprint arXiv:2405.20363*, 2024c.
 696

697 Zijie J. Wang, Evan Montoya, David Munechika, Haoyang Yang, Benjamin Hoover, and
 698 Duen Horng Chau. Diffusiondb: A large-scale prompt gallery dataset for text-to-image gener-
 699 ative models, 2023. URL <https://arxiv.org/abs/2210.14896>.
 700

701 Tobias Weyand, Ilya Kostrikov, and James Philbin. Planet-photo geolocation with convolutional
 702 neural networks. In *Proceedings of the European Conference on Computer Vision*, pp. 37–55,
 703 2016.

702 Magnus Wrenninge and Jonas Unger. Synscapes: A photorealistic synthetic dataset for street scene
703 parsing, 2018. URL <https://arxiv.org/abs/1810.08705>.

704

705 Zhipei Xu, Xuanyu Zhang, Runyi Li, Zecheng Tang, Qing Huang, and Jian Zhang. Fakeshield:
706 Explainable image forgery detection and localization via multi-modal large language models.
707 *arXiv preprint arXiv:2410.02761*, 2024.

708

709 Junyan Ye, Baichuan Zhou, Zilong Huang, Junan Zhang, Tianyi Bai, Hengrui Kang, Jun He, Honglin
710 Lin, Zihao Wang, Tong Wu, et al. Loki: A comprehensive synthetic data detection benchmark
711 using large multimodal models. In *ICLR*, 2025.

712

713 Xiaohan Zhang, Xingyu Li, Waqas Sultani, Yi Zhou, and Safwan Wshah. Cross-View Geo-
714 Localization via Learning Disentangled Geometric Layout Correspondence. In *Proceedings of
the AAAI Conference on Artificial Intelligence*, volume 37, pp. 3480–3488, 2023a.

715

716 Yue Zhang, Ben Colman, Xiao Guo, Ali Shahriyari, and Gaurav Bharaj. Common sense reasoning
717 for deepfake detection. In *European Conference on Computer Vision*, pp. 399–415. Springer,
718 2024.

719

720 Zhixin Zhang, Leqi Lei, Lindong Wu, Rui Sun, Yongkang Huang, Chong Long, Xiao Liu, Xu-
721 anyu Lei, Jie Tang, and Minlie Huang. Safetybench: Evaluating the safety of large lan-
722 guage models with multiple choice questions. *ArXiv*, abs/2309.07045, 2023b. URL <https://api.semanticscholar.org/CorpusID:261706197>.

723

724 Zhongliang Zhou, Jielu Zhang, Zihan Guan, Mengxuan Hu, Ni Lao, Lan Mu, Sheng Li, and
725 Gengchen Mai. Img2loc: Revisiting image geolocalization using multi-modality foundation
726 models and image-based retrieval-augmented generation. In *Proceedings of the 47th International
ACM SIGIR Conference on Research and Development in Information Retrieval*, pp. 2749–2754,
727 2024.

728

729 Sijie Zhu, Mubarak Shah, and Chen Chen. TransGeo: Transformer Is All You Need for Cross-view
730 Image Geo-localization. In *Proceedings of the IEEE/CVF Conference on Computer Vision and
Pattern Recognition*, pp. 1162–1171, 2022.

731

732

733

734

735

736

737

738

739

740

741

742

743

744

745

746

747

748

749

750

751

752

753

754

755